

# Spiking Neural Network based Water management in Drought Area of Maharashtra India: A Case Study of Osmanabad District

Devdatta K. Mokashi<sup>1\*</sup> and Prof. (Dr.) Vidula S. Sohoni<sup>2</sup>

Submitted: 19/11/2022

Revised: 21/01/2023

Accepted: 18/02/2023

**Abstract:** This paper proposes a machine learning technique for drought planning and risk reduction in agricultural regions dominated by smallholders. The proposed machine learning technique is Spiking Neural Network (SNN). Analysis of spatiotemporal features and patterns of meteorological drought at resolution is the major goal of the proposed control technique, which will help local risk planning and mitigation decisions as well as activities. Using publically accessible coarse scale data, the proposed method is employed in this study to produce high-resolution gridded precipitation products, which are then downscaled for investigation of meteorological droughts. Meteorological drought is defined by the Standard Precipitation Index (SPI). The purpose of the SNN for predicts the rainfall data resolution. By using coarse-scale precipitation data as a starting point for the high-resolution, spatiotemporal analysis of droughts, the proposed method is applied and adequately general to be adopted in other areas to enable local drought risk planning and targeted mitigation-decisions as well as movements. The proposed model is run on the MATLAB/Simulink platform, and the performance is evaluated using the existing methods. The proposed method helps to predict the drought and it has more success rate than the existing methods. The efficiency of proposed method is 0.9 which is way better than the existing techniques.

**Keywords:** Spiking Neural Network, Standard Precipitation Index, Drought Index, Metrological Drought Index, Drought Monitoring, Mean Drought Intensity, Drought Magnitude.

## 1. Introduction

In order to manage water resources, the components of the water balance must be precisely defined and regulated at various spatiotemporal scales [1]. Catchment processes are crucial for the study of the water cycle as well as hydrologic planning and management of water resources in a sink [2]. Precipitation, interception, evapotranspiration, runoff, infiltration, soil moisture, and groundwater flow make up the terrestrial water balance [3]. However, a number of water balance components are frequently hard to quantify, making this a difficult task. Additionally, changes in climatic conditions are likely to have an impact on how the water balance components are distributed spatiotemporally. [4] Global circulation models are frequently used in conjunction with various climate scenarios to study the climate change effects on several water balance components [5]. Additionally, numerous studies have used to forecast the changes in future projections. Utilizing a single raw GCM output results in insufficient comprehension, uncertainty in future projections, as well as biased climate projection outcomes [6]. The most recent GCN incorporates results

from phase-5 of the Coupled model inter-comparison project. The output-biased GSMs coarser resolution and its high level of parameterization are inappropriate for its application for the amount of water shed [7]. Using the biased-corrected and downscaled output from GCM, one can obtain information for the climate-change situations that are more accurate and have a finer resolution [8].

Recently, a number of local studies, NASA's Earth Exchange Global Daily Downscaled Projections dataset, which consists of statistically downscaled [9] output from 21 newer generation GCMs, has been shown to be useful for lowering uncertainty for both short- and long-term climate projections [10]. To examine the alterations in water balance components for future scenarios, hydrological models and downscaled climate models can be employed. Hydrological models are useful for quantitative knowledge of the numerous hydrological methods in a catchment [11]. As a result, these models are being used to inform management decisions and to study the climate change effects [12]. Selecting a hydrological model from the several available, selecting one models is very critical because of the desired [13] spatiotemporal resolutions and acceptable degree of error as well as uncertainty in the model imitations, data obtainability [14]. Hydrologists have developed sophisticated physically – based distributed models by improving the processing of spatial information as well as computational resources. A distributed method of hydrological modeling takes into account the geographical variability of various

<sup>1</sup>\*Research Scholar, Bharati Vidyapeeth (Deemed to be) University, College of Engineering, Pune-411046, India  
<sup>2</sup>Principal, Bharati Vidyapeeth College of Engineering, Bharati Vidyapeeth (Deemed to be) University, Pune, India  
\*Corresponding Author ORCID ID: 0000-0002-0560-3658  
\* Corresponding Author Email: dev.mokashi@gmail.com

hydrological methods in a catchment by grid-wise distribution of model parameters [15], as well as catchment characteristics and metrological forcing. As a result, they are favored over grouped models. The VIC models are macro scale hydrological models with a physical foundation that deal with the better depiction of horizontal-resolution utilizing sub-grid variability of soil-moisture storage, land usage, and other factors. For an improved graphic depiction of precipitation and environmental lapse rate, nonlinear base-flow representation and topography inclusion are used [16]. In the past, the VIC models are employed for hydrological simulations of various catchment sizes and provided accurate estimates of the various hydrological processes [17].

The effects of droughts on the agricultural, industrial, and social sectors are extensive. On 38% of the world's land surface, there are nearly 70% of people who are at risk of drought [18]. Due to their gradual development, sluggish onset, and protracted length, droughts are also more challenging to detect and anticipate. Drought dynamics must be better understood over a long period of time, to plan and direct mitigation efforts. There are three types of droughts: meteorological, socioeconomic and agricultural [19]. A meteorological drought is caused by rainfall that is below a certain threshold, and it is followed by agricultural, hydrological, and socioeconomic droughts when it persists for long periods of time. Drought indicators include precipitation, soil moisture, stream deficiency [20], and groundwater table, all of which have different response times. The socioeconomic drought is produced by the combined effects of agricultural, meteorological, and hydrological drought conditions, putting millions of people's food and water security at risk. This study focuses on high-resolution, spatiotemporal studies of meteorological droughts. Drought duration, severity, intensity, and frequency are all quantitative metrics that have been used to define, quantify, and track droughts [21]. These are based on the notion that a drought is a series of time-intervals with an index-value less than a predetermined threshold.

In this paper proposes a machine learning technique for drought planning as well as risk mitigation in predominantly small-holder agriculture-areas. The proposed machine learning technique is Spiking Neural Network (SNN). The proposed control technique's main goal is to analyze the spatiotemporal features and patterns of meteorological drought at resolve in order to enable local risk planning and mitigation decisions as well as activities. Section-1 describes the introduction of the paper. Section-2 explains about the recent research work. Section-3 discuss about the configuration of this paper. Section-4 deeply discuss about the proposed technique used in this paper which is SNN. Section-5 discuss about the results

obtained by using the proposed method. Section-6 accomplishes the paper.

## 2. Recent Research Work: A Brief Review

Numerous research works have earlier presented on the literature which is depends on the machine learning technique for drought planning as well as risk mitigation in mostly small holder agriculture-areas utilizing different methods and features. Here, some of them are revised.

Zhou et al., [22] have proposed the primary objectives of characterizing agricultural drought and examining the relationships between meteorological, agricultural, and vegetation droughts after evaluating the utility and applicability of the combined SM product and the monthly scaled soil water deficit index (SWDI). According to Hossain et al., [23], making water accessible for agricultural, drinking, residential, and other uses, as well as for other purposes, and ultimately for the survival of flora and fauna, was the primary priority of the Barind Tract (BT), which is located in northwest Bangladesh. The BT's continuous groundwater level (GWL) depletion was primarily caused by excessive groundwater extraction for irrigation, low rainfall, and fewer sources of surface water, high temperatures, and thick top clay that inhibits natural recharge. As a result, the region's lithology and groundwater condition required the modified managed aquifer recharge (MAR) method. Hiloidhari et al., [24] have presented Sugarcane bagasse-based cogeneration contributes considerably to bioenergy conversion in India; consequently, suitable performance study taking regional characteristics into account was required. With the government's aim to raise the share of renewable energy by 2030, more sugarcane bioenergy was predicted in India.

Neeti et al., [25] have created an integrated system for generating high-resolution gridded precipitation products from publically obtainable coarse-scale data and analyzing meteorological droughts using the downscaled products. The framework was developed and tested using data from a part in Central India. Meteorological dryness was defined using the Standard Precipitation Index (SPI). Quintana-Segu et al., [26] have established a drought diagnosis and forecasting system to address fundamental difficulties in hydrological management in Spain, where recurring water scarcity times were common. Land-surface models (LSMs) could offer water managers with useful information on how drought conditions emerge. Ahmed [27] have examined the effects of drought-driven agricultural policy as well as projected climate change on the performance of major irrigation systems in SSA, with a focus on the Gezira scheme, GS (0.88 mha) in Sudan. However, severe and moderate drought events will continue to be a problem until 2060. The quantification of water-budget components was a crucial step in the

planning and management of water resources in all river basins was created by Nandi and Manne [28]. Numerous studies have demonstrated that the hydrology of the Earth will be impacted by climate change. The water balance components in the Sina basin, which is prone to drought, are simulated using the VIC (variable infiltration capacity) model.

### 2.1. Background of Recent Research Work

A review of recent study work demonstrates that water management in drought areas and crisis resolution. Existing drought monitoring systems provide data on drought indicators at the regional level. The absence of in-situ meteorological/hydrological or soil moisture observing networks has made drought monitoring at smaller scales more challenging. It is both time-consuming and labor-intensive. Though, in recent years, satellite-based gridded precipitation products have offered a useful alternative for ongoing drought monitoring. These products have slightly higher spatial resolutions (0.25 to 1; 25 km to 100 km). They include the Multi-Satellite Precipitation Analysis (TMPA), Tropical Rainfall Measuring Mission (TRMM), Precipitation Estimation from Remotely Sensed Information Using Artificial Neural Networks (PERSIANN) and others. With a spatial resolution of 0.05 (5 km), the Climate Hazards Group Infrared Precipitation

with Stations (CHIRPS) rainfall gridded, which employs a Random Forest algorithm with satellite-derived indices EVI, elevation, feature, and latitude as cofactors, has a higher spatial resolution than other current satellite data-based gridded precipitation products. The prediction is based on CHIRPS (5 km) monthly precipitation data with a 1 km resolution and ANN methods. Although they did not investigate drought concerns at this level, this study concentrated on spatial downscaling of rainfall to 1km. This research project is motivated by these issues and concerns.

### 3. Configuration of the Water Management in Drought Area

This section defines the proposed method for the water management in drought area in Maharashtra. Main goal is to select the proper Drought indices (SPI). By selecting the proper indices, the correct regions with different climates can be found [22]. Analyzing the water management in drought in Maharashtra and analyzing the variation of rainfall across the state [23]. The proposed methods help in predicting the droughts and find the region which is greatly affected by drought. Figure 1 shows that the Structure of water management and prediction of drought using proposed algorithm.

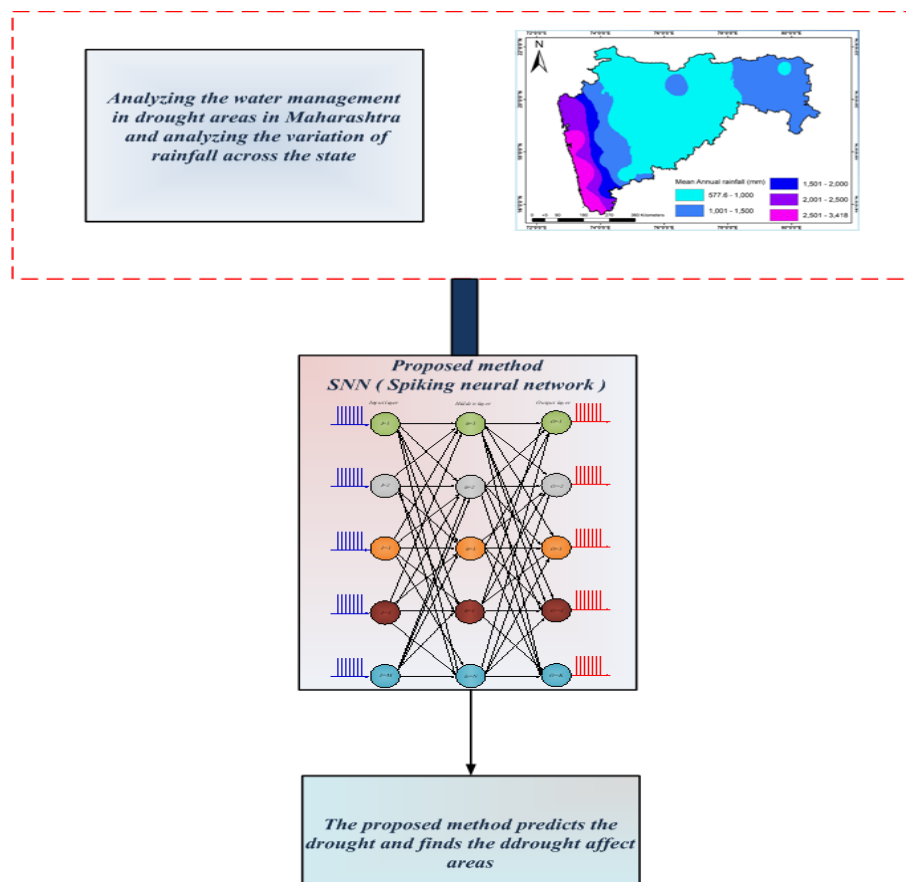


**Fig 1:** Structure of water management and prediction of drought using proposed algorithm

Using proper machine learning models is very essential in managing the drought Figure 1. The meteorological variables like rainfall, temperature, wind speed, relative humidity, are required in predicting the droughts [24]. The selection of best model parameters and testing the model

can be useful in predicting the drought. Comparing the prediction accuracy of the models helps to differentiate between the proper models to help in predicting the drought [25]. The methods and prediction of drought is displayed in Figure 2

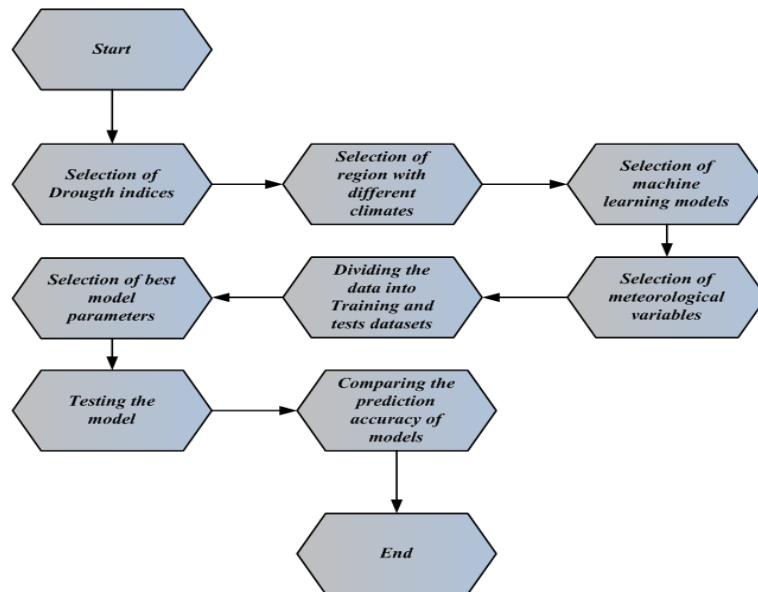


Fig 2: Method and analysis of prediction of drought

### 3.1. Overview of Drought in Maharashtra

Each year, significant effects of droughts are felt in one or more regions of India. A water shortage of varying severity affects almost all of the states in the union. More than 300 districts in India are thought to be particularly susceptible to the severe effects of droughts, which affect more than 60% of the population [26]. Maharashtra, a state in central India, virtually always experiences drought in some capacity. The state's rainfall pattern exhibits considerable geographical and temporal variance. The average amount of water in Maharashtra is 198 billion cubic meters

(BCM), and the majority of the population of state depends on agriculture for a living. The main purpose is to examine the return period, intensity, as well as persistence of droughts across Maharashtra's numerous districts in order to find measures to alleviate the drought crisis in the future [27]. About 42.5% of Maharashtra's land area is in sub basins with deficiency and very deficit water supplies, and it frequently experiences droughts. The state's significant population is impacted by the repeated drought episodes throughout the state, which result in enormous losses to agricultural productivity [28]. Figure 3 displays the Systematic analysis of Rainfall and Analysis.

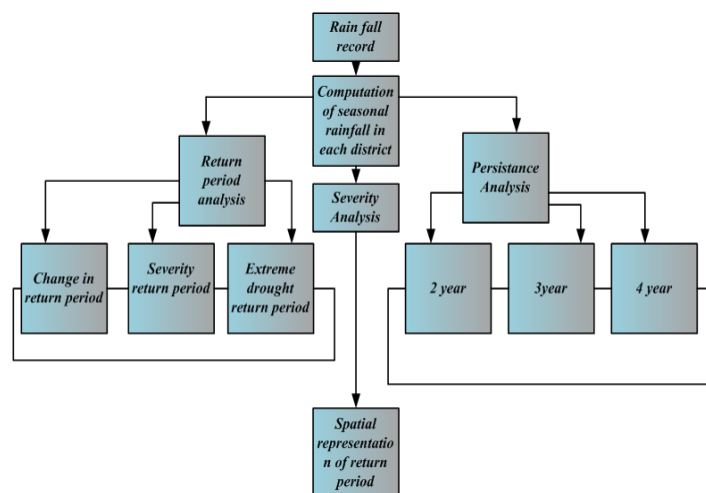
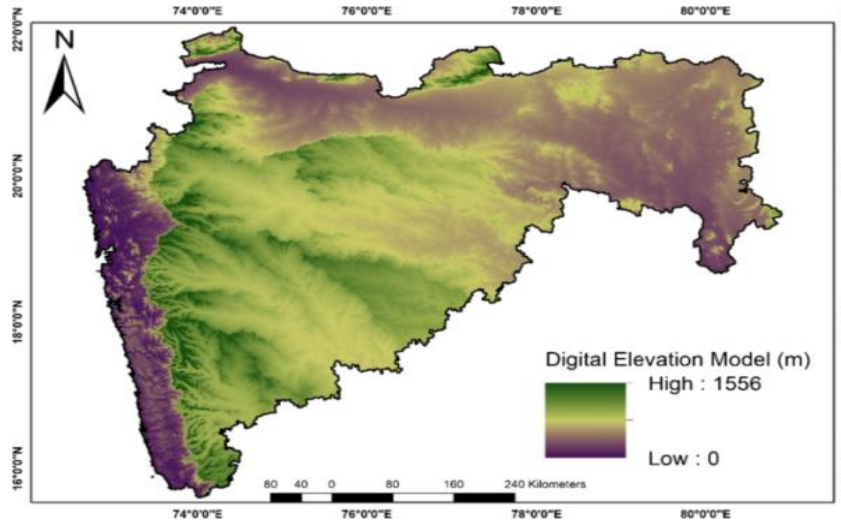


Fig 3: Systematic analysis of Rainfall and Analysis

The Maharashtra is situated in India's western region. The state capital is Mumbai. The state is almost 307,713 km<sup>2</sup> and it is one of the largest states of India and the overall population is around 128 million. Maharashtra is divided in 6 major divisions Nasik, Amravati, Konkan, Aurangabad, Pune and Nagpur division. The state's western region is surrounded by coastline of 720 Km of long coastline [29]. Madhya Pradesh, Chhattisgarh, and Karnataka surround Maharashtra. The districts which are surrounded by the

coast receives a high amount of rainfall more than 2000 mm yearly the districts like Pune, Nasik, Dhule, Kolhapur, Sholapur receives less than 600 mm of rainfall yearly [30]. The state experiences a hot summer with temperature ranges between 22°C and 43°C. The state's forest area is approximately 61,939 km<sup>2</sup>, accounting for 20.13% of state's geographical region; agriculture in state is primarily dependent on rain [31]. The state's digital elevation model (DEM) is shown in Figure 4.



**Fig 4:** The digital elevation model (DEM)

Figure 5 depicts variation in annual rainfall across the state, which is collected from the Indian metrological department pune [32]. The average rainfall in the state differs from 577 mm to maximal of 3418 mm. the people are majorly affected due to the lack of rainfall and affects the people in their day to day life. This paper makes use of monthly rainfall data from 1901 to 2013. Rainfall statistics

for 34 districts are attained from the IMD, Government of India, and Pune. States receive about 80% of yearly rainfall at the monsoon season. The departure from monsoon rainfall has been computed for every district in the state in order to recognize drought years as well as assess the severity of the events [33].

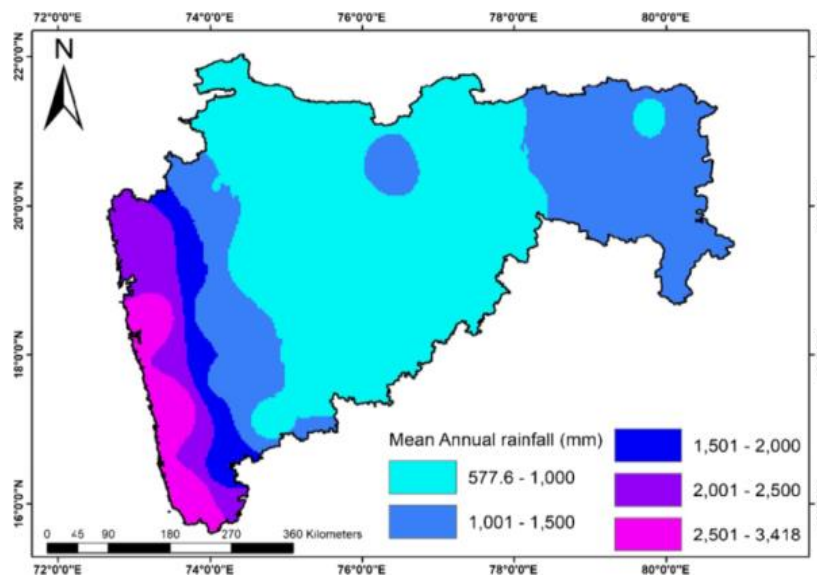


**Fig 5:** Variation in annual rainfall across the state

Drought episodes are divided into three types based on the mean seasonal rainfall deviation: moderate drought, extreme drought, and severe drought. According to IMD drought in a year is classified on the basis of low seasonal/annual rainfall from the previous consistent year average is more than 25%. The drought is categorized as severe, moderate and extreme on based on low rainfall. To identify drought years, the variance in yearly monsoon rainfall from the corresponding average is computed and reported in every district of the state. The drought return period is calculated by comparing the net count of rainfall ratio to the count of drought years [34].

$$T^{\frac{1}{4}} N = n \quad (1)$$

here the net count of years of analyzed rainfall represents N, the return period denotes T, the net count of years with rainfall deficiency of greater than 25% denotes n. [35]. Extreme and severe droughts have been determined, as well as their return periods [36]. A prolonged drought occurrence occurs when a drought lasts for two or more years.

### 3.2. Categorization of Droughts

In this study, the SPI drought index is primarily utilized to define droughts throughout time. The SPI is a widely used metric for characterizing droughts. SPI characterizes droughts by taking into account both precipitation and potential evapotranspiration [37]. Therefore, SPI considers not only the influence of variations in precipitation but also the impact of temperature on droughts. Droughts are divided into three groups in this study depends on their intensity as designated by SPI as moderate-drought, severe-drought, and extreme-drought [38].

### 3.3. Droughts Prediction

Drought prediction models are evaluated using the final set of predictors' SPI data. The models are then validated using SPI data from the final sets of predictors matching the timeframe. The three drought classifications are projected to last between 1-6 months SPI [39]. The most effective selection of its hyper-parameters, like the SNN weight, is crucial for ML-based models' success. To ensure the model is calibrated and authenticated with all observations, the method is performed five times, every time with a fresh sub-sample [40]. The final model's optimal values are then determined by using the hyper-parameter's average values [41]. There is no general guideline for choosing the optimal value of k. Typically, it is decided through trial as well as error. In the current investigation, setting the value of k led to the best calibration and validation outcomes. The appendix provides a summary of the current state of learning

algorithms, SNN, used to create drought prediction models [42].

### 3.4. Severity of Drought Events

This paper, the rainfall deviation from long term average is elaborated in terms of severity. The degree of the seasonal rainfall deficit from the average is another word for the severity. For every district, the seasonal rainfall shortfall is computed. Every district's seasonal rainfall has been computed with a maximum deviation [43]. It basically helps us to help to identify the severity of drought in each district and also it can identify the lack of rain fall in drought severe districts, it can help in reducing the drought in each district by using the proper drought controlling method.

### 3.5. Composite Effective Meteorological Drought Index

In order to identify regional patterns of drought vulnerability for the spatial targeting of drought policies as well as mitigation measures, it can be very helpful to develop a composite index that associations the effects of various drought features such as intensity, severity, duration, and frequency into a single "effective meteorological drought index" [44]. Applying SPI to the various drought characteristics provides such an indicator.

### 3.6. Analysis of Drought Detection

Different operational drought indexes are created. The SPI, one of the several drought indices, is frequently employed [45]. The standardized precipitation evaporation index (SPEI), the most current drought- index to be created, highlighted the significant impact of the selected drought index as well as time scale in scaling drought occurrences [46]. The attribute to the PDSI formula and the datasets used to estimate evapotranspiration for the results that are in conflict with the relationship between drought and climate change. It is determined that the SPI is the best index for the Maharashtra region. When compared to SPEI, the SPI distinguishes itself by having more time flexibility and fewer input requirements.

### 3.7. Standard Precipitation Index (SPI).

The SPI is equipped to manage the consequences of drought events. WMO (World Meteorological Organization) has validated this indicator. Only precipitation data are required for SPI calculations. It is utilized to calculate the precipitation deficit over a range of time periods, involving 48, 24, 12, 6, 3, and SPI-1 months. Here, using the rainfall data, individual SPI is computed in R-environment.

$$SPI = \frac{X_i - \bar{X}}{\sigma} \quad (2)$$

here Precipitation of the station represents  $X_i$ , Standard Deviation represents  $\sigma$ , Mean precipitation represents  $\bar{X}$ . To characterize the intensity of the occurrence of drought in Maharashtra for the purposes of the current research, only the extreme and severe drought classifications are considered. Depending on SPI values for drought categorization, the classification of drought is employed. The duration of SPI is utilized in the study because it more accurately reflects long-term precipitation conditions and may be used to compute stream-flows, groundwater-levels, as well as reservoir-levels. Extreme and severe drought frequency is computed as percentages.

$$N_{i,100} = \frac{N_i}{i, n} \times 100 \quad (3)$$

here  $N_i$  signifies the many months with droughts for a time scale  $i$  in  $n$  year set,  $N_{i \times 100}$  represents the many drought for a specific timeframe  $i$  in 100 years,  $i$  signifies time scale. Drought-magnitude is the CWS (cumulative water scarcity) at the drought time as well as MID (means drought intensity) is the average of this CWS for the drought-period, hence MD and MID are comparable.

$$MD = \sum SPI_{ij} \quad (4)$$

$$MID = \frac{MD}{m} \quad (5)$$

here  $m$  denotes number of months and SPI denotes the SPI values for a specific drought spell within the  $j$  timeframe. All SPI values are initially organized in ascending order for the purpose of calculating the recurrence interval, and all positive SPI values are then given the number 0. For the final step in calculating the RI of severe and extreme drought, the California technique is used.

$$RI = \frac{n}{Er} \quad (6)$$

here the order or rank of the event represents  $Er$ , the number of events represents  $n$ . Linear regression is used to determine the rainfall trend. The critical or threshold rainfall can be determined using

$$CR = \sigma SPI + \bar{X} \quad (7)$$

where  $\sigma$  represents the Standard Deviation,

### 3.8. The SPI Drought Index

The drought occurrences are identified and analyzed using the standardized precipitation index (SPI). In order to analyze SPI, total precipitation for the stations of interest is fitted with a probability density function (PDF), and the gamma-distribution is used, requiring an estimate of its corresponding  $\alpha$ ,  $\beta$ -parameters for every timescale of

interest (1, 2, 3 months) as well as for every month of the year. Frequency of the gamma-distribution, or

$$G(x) = \int_0^x g(x) dx = \frac{1}{\beta^\alpha \Gamma(\alpha)} \int_0^x x^{\alpha-1} e^{-x/\beta} dx \quad \text{for } x \geq 0 \quad (8)$$

where shape and scale parameters represents  $\alpha$  and  $\beta$ , precipitation amount represents  $x$  and the Gamma function represents  $\Gamma(\alpha)$ . Maximal probability solutions are applied to validate  $\alpha$  and  $\beta$ . These parameters, sometimes referred to as the resultant parameters, are utilized to calculate the SPI values by calculating the cumulative probability of an perceived precipitation event over the given month as well as period in the given station [47, 48]. The severity of drought or non-drought episodes is then determined by dividing the produced SPI values into several categories of above and below normal values. Based on the SPI analyses, other drought features, like duration, magnitude or intensity, may be determined. In a sample set, multiple zero values are also possible. The CDF for the Gamma-distribution is different as follows to take into account the zero-value probability:

$$H(x) = q + (1 - q)G(x) \quad (9)$$

here the probability of zero-precipitation represents  $q$ . In order to determine the SPI values, the computed precipitation probabilities are converted into the matching standard-normal values.

### 3.9. Validation of Predicted Rainfall

Forecasts for climate-change indicate likely future scenarios based on a variety of presumptions. Many climate change modelers define stationary as "the climatic variable troubled has a time-invariant probability density function whose properties may be assessed from instrument record and errors are reducible by extra observations," making validation of future scenarios difficult and contentious. Because of inadequate climate knowledge and perceived datasets, many climate-change modelers assumed stationary in time series. In accordance with this, the simplest method for determining if or not observed and demonstrated precipitation follow the similar specified theoretical model is to statistically test this

$$D = \max[CDF_o - CDF_{cori}] \quad (10)$$

The bias correction rate, BCR, is used to assess the degree to which the methodologies used have produced actual indications of climatic change. This ratio contrasts how much the medians changed over the course of the observed and modeled timeframes.

$$BCR = \frac{O_P^E - O_{0.5}^E}{M_P^E - M_{0.5}^E} \quad (11)$$

here the early period is denoted by E, the median by 0.5, and the percentile (P≠0.5) value of the novel-model median in old-model distribution by p.

### 3.10. Selection of the Climate Domain

The synoptic climate that affects temperature and precipitation over the study region of interest is frequently used to determine the aerial extent of the climate domain for predictor selection. The domain's size should be just right-not so small that air phenomena might not be detected or too big that computing would take longer and cost more. Therefore, choosing a suitable climate domain is crucial for accurately forecasting droughts. This research investigates a climate domain restricted by latitudes 0-100E and longitudes 10-40 N, taking into account the effect of air circulations responsible for droughts.

### 3.11. Agricultural Drought Inventories

A thorough agricultural drought inventory is created using the relative departure of soil moisture since low soil moisture is a key sign of agricultural-drought. While a given crop's absolute soil moisture threshold can be used to map agricultural drought, crop types range greatly between regions with varied climates, thus farmers may choose more drought-resistant crops in dry places. We therefore suppose that for a large range of mean annual precipitation, which is a useful indication of agricultural drought.

### 3.12. Sensitivity Indicators

As a result, we believe that average temperature, proportion of small farmers, total water usage, net sown area, potential evapotranspiration, crop water demand, cultivable area, cropping intensity, and population density are reliable indicators of agricultural productivity in our current work. These factors influence how people respond to exposure dangers. For instance, a region becomes more vulnerable to drought as a result of increased population pressure since more people live there. The most significant meteorological variables that affect land cover, water balance, and ecological sustainability are temperature and potential evapotranspiration. This group of sensitivities covers economic and biophysical aspects.

### 3.13. Resilience Indicators

The incapacity of a certain demographic group to appropriately respond to a particular harmful stimulation is referred to as vulnerability. Because of this, the social vulnerability of social group is determined by its inability to respond to a potential threat. The socioeconomic resilience indicators, such as fertilizer usage, water availability, income index, health index, forest area, net irrigated area, education index, and are therefore involved in this work [49]. These variables reflect a population's

capability to withstand stress, or, to put it another way, its capacity to adapt to or recover from a drought. For instance, the amount of forest cover will reveal the region's level of greenery and, consequently, the degree to which the public and the government are prepared for drought shocks.

### 3.14. Exposure Indicators

These variables aid in determining the extent of the drought's impact on the region or its inhabitants. Severe drought-frequency (%), extreme drought-frequency (%), annual precipitation, rainfall trend, mean drought-intensity, repetition interval of extreme-drought, critical rainfall, drought magnitude, recurrence interval of severe-drought, and wet-day frequency are the indicators used to represent exposure. The SPI is used to compute extreme and severe drought rates, MID, MD, and repetition intervals of severe and extreme drought [50].

### 3.15. Performance Assessment

The drought prediction models' performance is evaluated utilizing 4-different statistical indices. The co-efficient of determination ( $R^2$ ) varies between 0 and 1. The range of normalized root mean squared error is 0 to +. The bias percentage ranges from - (underestimation) to + (overestimation), with 0 denoting complete agreement.

$$R^2 = \frac{\sum_{i=1}^N (O_i - \bar{O}) \cdot (S_i - \bar{S})}{\sum_{i=1}^N (|S_i - \bar{S}|)^2 \sum_{i=1}^N (|O_i - \bar{O}|)^2} \quad (12)$$

$$NRME = \frac{\sqrt{\frac{1}{N} \sum_{i=1}^N (S_i - O_i)^2}}{sd(O_i)} \quad (13)$$

$$PBIA S = 100 \cdot \frac{\sum_{i=1}^N (S_i - O_i)}{\sum_{i=1}^N (O_i)} \quad (14)$$

$$md = 1 - \frac{\sum_{i=1}^N (O - S_i)^j}{\sum_{i=1}^N (|S_i - \bar{O}| + |O_i - \bar{O}|)^j} \quad (15)$$

## 4. Spiking Neural Network (SNN) Based Water Management in Drought Area

Water management in drought areas is evaluated using the Spiking Neural Network method that is described in this research. The term SNN is used in work to refer to any type of NN that incorporates time as well as neuronal and synaptic states. In particular, the spiking neural model's synaptic weight can be automatically adjusted using the SNN algorithm during the learning phase. SNN offers a superior solution model for balancing exploration and exploitation, according to various application data [51]. The method by which data is indicated by spike trains is



referred to as neural coding. The techniques for encoding real values include population, rate, and temporal encoding. The connected temporal events concealed inside the sequence are thought to be exploited in a temporal neural coding system suitable to sequence Modelling and predicting applications. Times to next spike as well as probability-based encoding are included. It continuously feeds information into the network at the precise time of spikes. Spike trains, the input and output of spiking neurons, are signified by firing time series. The potential of a spiking neuron is signified by a dynamic variable that functions as an incorporator of arriving spikes, with fresher spikes having a greater impact than older spikes on net action potential. A dynamic variable that serves as an incorporator of arriving spikes serves as a representation of a spiking neuron's potential, with more recent spikes having a stronger influence on net action potential than older spikes.

#### 4.1. Fundamental Theories of Supervised Learning For SNNs

Commonly, structure of supervised learning Spike train spatiotemporal pattern learning is utilized to implement supervised learning for SNNs. In time-interval  $\Gamma = [0, T]$ , spike-train  $s = \{t \mid f \in \Gamma: f = 1, \dots, F\}$  is the ordered-sequence of spike-times that spiking-neuron fire, and it can be stated as follows:

$$s(t) = \sum_{f=1}^F \delta(t - t^f) \quad (16)$$

here  $F$  represents the count of spikes,  $t^f$  represents the  $f$  spike time in  $s(t)$ ,  $\delta(\cdot)$  signifies the Dirac delta function:  $\delta(x = 1)$  if  $x = 0$ ,  $\delta(x = 0)$  or else. Determining the proper synaptic-weight matrix  $W$  for spiking neural networks to create the real output spike-trains  $S_a$  as equivalent to the consistent preferred output spike-trains  $s_d$  as possible, i.e., to make the difference in the error value estimation function  $E(S_a, S_d)$  among them is a minimal, is the general objective of the various supervised learning algorithms for spiking-neural networks. In the supervised learning method, the result spike-trains  $S_a$  is formalized as being affected by the input spike-trains  $S_i$  as well as the synaptic-weight matrix  $W$  associated with them.

$$s_a = F(S_i, W) \quad (17)$$

Here  $F$  denotes functional relationship among  $S_i$  and  $W$ ; hence, supervised learning for spiking neural networks may be expressed by

$$\min E(S_a, S_d) = \min \sum_{m=1}^{N_o} |S_d^m(t) - S_a^m(t)| \quad (18)$$

here  $N_o$  denotes count of output neurons, and  $|S_d^m(t) - S_a^m(t)|$  denotes similarity distance among  $S_d^m(t)$  and  $S_a^m(t)$ . Accordingly, supervised-learning is a method of reducing the network's overall error, where the error can be calculated using the similarity of spike-trains. The overall structure of supervised-learning for the SNN, supposing that SNN has  $N_i$  input neurons as well as  $N_o$  output neurons.

#### 4.2. Computational Models of Spiking Neurons

Spiking neurons are the essential computational components of spiking neural networks. It is critical to create proper spiking neuron models in order to replicate nervous system operation and solve genuine issues utilizing spiking neural networks. Depending on complexity, the spiking neuron computational method can be split into three groups: Physiological models with biological plausibility, non-linear models with a spiking mechanism, and linear models with a set threshold are all examples of such models. The integrate-and-fire neuron model and the spike response model using analytic expressions are two simple spiking neuron models are frequently utilized in spiking neural network simulation, particularly in supervised learning, whereas others, like the Hodgkin-Huxley model, are too complex for large-scale SNN simulation.

#### 4.3. Simulation Strategy for SNNs

Simulation of SNNs differs from that of typical ANNs as the spiking-neuron is signified as a hybrid-system by the constant method as well as distinct spike occurrences. For SNNs, two simulation approaches are typically used: a clock-driven simulation approach and an event-driven simulation approach. The quantitative way to determine the similarity degree among spike trains is the similarity measure. Different measurement techniques have already been offered by researchers. To compute errors in the supervised learning method of spiking neural networks, parallel measurements among actual as well as intended output spike-trains are required. On the one hand, supervised learning accuracy is calculated by calculating spike train errors, and while the error is less than a predefined value, the learning iteration method is terminated. In contrast, learning rules of a few controlled learning algorithms are produced using a predetermined specified error function.

#### 4.4. The Architecture of Single-Layer spiking neural network

The special feed-forward spiking neural networks is known as single-layer SNNs. There are no hidden-layers and there is one input and output-layer. In single-layer SNNs, there

is single-layer of synaptic-weight. Therefore, supervised learning is actually for spiking neurons rather than single-layer spiking neural networks. Single-layer SNN has a

straightforward construction and is frequently used in SNN simulation. Figure 6 depicts Construction of a single-layer SNN.

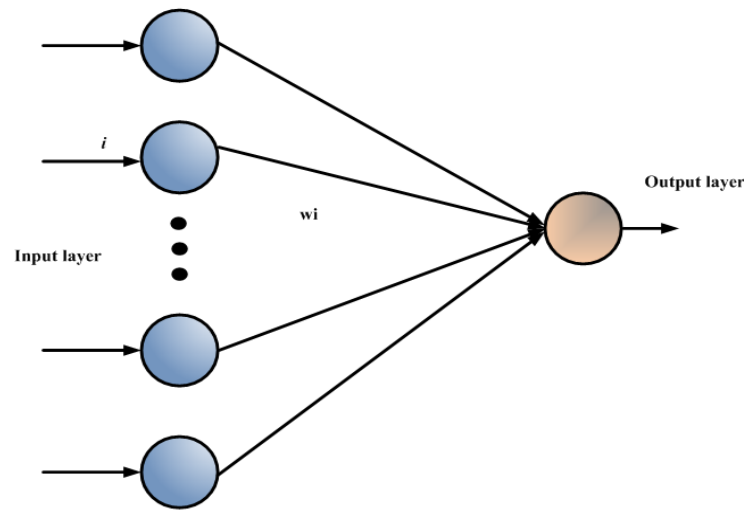


**Fig 6:** Construction of a single-layer SNN.

#### 4.5. Supervised Learning for Multi-layer Feed-Forward spiking neural networks

A several-layer feed-forward spiking neural network is one of spiking neural networks architectures that are frequently utilized. A multi-layer feed-forward SNN's neurons is organized hierarchically. Only the neurons in layer below are coupled to every neuron. The input-layer of the spiking neural network is the first-layer. This layer serves as the

SNN's input and does not include any neuronal computation. A spike-train of every input layer neuron, which is fed into the SNN's next layer, indicates the coding of input-data for the precise issue. As pike-train that every neuron in final layer, or output layer, fires represents the network's output. There could be one or more hidden-layers among the output and input-layers. Figure 7 depicts construction of a multi-layer feed-forward spiking neural network.

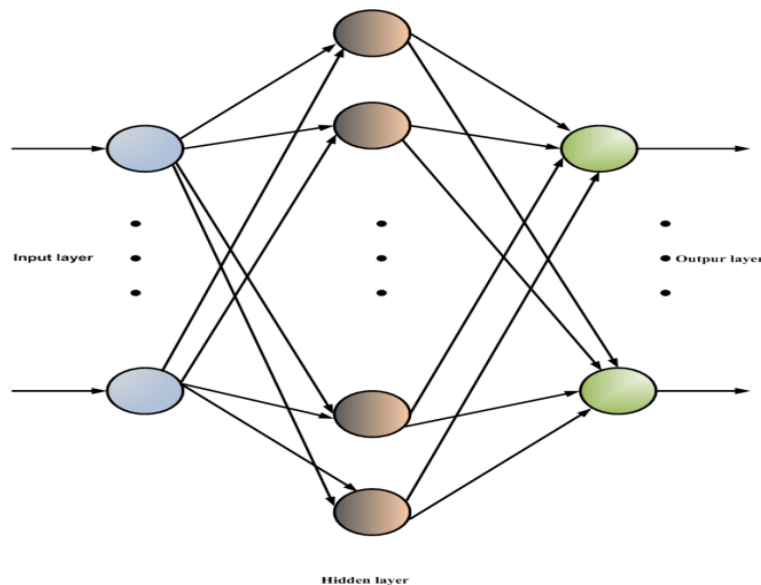


**Fig 7:** Construction of a multilayer feed-forward SNN

### 5. Result and Discussions

This section the proposed approach performance based on the simulation outcome. In this paper the SNN is utilized.

The proposed approach performance is Implemented in MATLAB / Simulink platform and related with existing methods. The proposed approach is analyzed under

different circumstances and it concludes that the proposed technique is better than the existing methods.

Comparison of predisposing factors of Districts (a) Gadchiroli and (b): Gondia is shown in Figure 8. The predisposing factors are 1.Rainfall trend, 2.Annual rainfall, 3.Critical rainfall, 4.Wet day frequency, 5.Drought magnitude, 6.Mean drought intensity, 7.Severe drought frequency, 8.Frequency of extreme-drought, 9.Return period of severe-drought, 10.Return period of extreme-drought, 11.Potential evapotranspiration, 12.Average temperature, 13.percentage of small farmers, 14.Net sown region, 15.Cropping intensity, 16.Water availability, 17.Total water use, 18.Crop water demand, 19.Forest area, 20.Population density, 21.Net irrigated region,22.Cultivable area, 23.Education index, 24.Income index, 25. Fertilizer consumption, 26.Health index. Subplot 8 (a) depicts the factors of district Gadchiroli in which the Annual rainfall is about 1 and the returning period of extreme-drought is about 1. The water availability is around 1 and the total water usage is about 0.9, the forest area is about 0.8. The health index is about 0.5, and the fertilizer consumption is about 0.5. Subplot 8(b) depicts the predisposing factors of district Gondia. The Rainfall trend is about 0.2 and the mean drought intensity is about 0. The average temperature is around 0.9. The cropping intensity is about 1 and the cultivable area is about 0.5, the fertilizer consumption is around 0.8. Analysis of predisposing factors of districts (a) Bhandara & (b) Chandrapur is shown in Figure. 9. Subplot 9(a) depicts the predisposing factors of district Bhandara in which the Annual rainfall reaches an overall value of 1 and the wet day frequency is about 0.8. The critical rainfall is around 0.1, the severe drought frequency is about 0.7, the average temperature is about 0.5. The water availability is about 0.9. The crop water demand is about 0. The value of income index is about 0.3 the value of fertilizer consumption is around 0.9. Subplot 9(b) depicts the predisposing factors of district Chandrapur. The value of drought magnitude is 0.8, the potential evaporation is around 0.6, and the value net sown area is 0.2, the value of water availability is around 0.9 the total water usage is around 0.8, the value of net irrigated area 0.2, the cultivable area is around 0.4. The value of fertilizer consumption is 0. Comparison of predisposing factors of districts (a) Yavatmal & (b) Wardha is shown in Figure. 10. Subplot 10 (a) depicts the predisposing factors of district Yavatmal. The annual rainfall value is about 1 and the rain fall trend is 0.4, the wet day frequency is about 0.8, the return period of extreme drought is about 0.9, the water availability is about 2. The total water usage is about 1. The net irrigated area is about 0.4. In subplot 10(b) depicts the predisposing factors of district Wardha. The Annual rainfall is about 1, The Critical rainfall is around 0.1. The mean drought intensity is 0.1. The severe

Drought frequency is at 0.8. The water availability is at 1. The total water usage is at 0.9. The net irrigated area is at 0.8. The fertilizer consumption is at 0. Analysis of predisposing factors of districts (a) Osmanabad (b) Latur is shown in Figure. 11. Subplot 11(a) Depicts the predisposing factors of district Osmanabad. The Annual Rainfall is about 1. The rainfall trend is at 0.2, the wet day frequency is at 0.9. The value of critical rain fall is at 0.1, the mean drought intensity is at 0.1, the value of drought magnitude is about 0.2, and Extreme drought frequency is about 0.6. The severe drought frequency is at 0.7, the average temperature is around 0.9. The water availability is at 1, the total water usage is about 1, and the cultivable area is about 0.3 Subplot 11(b) depicts the predisposal factors of district Latur. The annual rainfall is about 0.7 and the Rainfall trend is about 0.8, the wet day frequency is about 0.5, the value of critical rainfall is about 0.2. The water availability is at 1.1.the total water usage is about 1. The fertilizer consumption is around 26. Analysis of predisposing factors of districts (a) Sangli& (b) Solapur is shown in Figure 12. Subplot 12(a) depicts the pre disposing factors of district Sangli. The annual rainfall of the District is about 0.9. The Rainfall trend is about 0.3. The wet day frequency is about 0.8. The mean drought intensity is around 0.1, the drought magnitude is around 0.9, the extreme drought frequency is at 0.1 and the severe drought frequency is at 0.8, the water availability is at 1, the total water usage 1. The cultivable area is around 0.6 and the fertilizer consumption is at 0.7. Subplot 12(b) depicts the predisposing factors of district Solapur. The annual rainfall value is about 0.5, the rainfall trend is about 0.6, the wet day frequency is about 0.1, the value of critical rainfall is 0.4, the mean drought intensity is at 0.1, and the drought magnitude is about 0.8, the returning period of extreme-drought is 0.8. The potential evapotranspiration is 0.5, the water availability is at 1 and the total water usage is around 1 the net irrigated area is about 0.9, the fertilizer consumption is around 0.8. Analysis of predisposing factors at districts (a) jalgaon and (b) Ratnagiri is shown in Figure 13. Subplot 13(a) depicts the predisposing factors of district jalgaon. The annual rainfall value is at 1 and the rainfall trend is about 0.4, the wet day accuracy is around 0.6 the critical rainfall is about 0.1, the mean drought intensity is at 0.02, the drought magnitude is about 0.9, the extreme drought intensity is at 0.3 , the severe drought intensity is at 0.4, the returning period of severe-drought is at 0.8 , the returning period of extreme-drought is at 0.9, the average temperature is at 0.5, the potential evapotranspiration is at 0.8, the net sown area is at 14 ,the water availability is at 1, the fertilizer consumption is at 0.9 . Subplot 13(b) depicts the predisposal factors of district Ratnagiri. The annual rainfall is at 0.1, the wet day frequency is at 0.1, the mean drought intensity is at 0.02, the drought magnitude is at 1, the extreme drought intensity is at 0.2, the severe drought intensity is at 0.8, the

water availability is at 1 and the total water usage is at 0.9. Analysis of predisposing factors of districts (a) Sindhudurg&(b) Dhule is shown in Figure 14. Subplot 14(a) depicts the analysis of predisposing factors of District Sindhudurg. The annual rainfall is about 0.8, the Rainfall trend is at 0.6, the wet day frequency is at 0.3, the critical rainfall is around 0.1, the mean drought intensity is at 0. The drought magnitude is at 0.9, the extreme drought intensity is at 0.5, the severe drought magnitude is at 0.9, the water availability is at 1, the total water usage is at 0.9, the fertilizer consumption is at 0.6. Subplot 14(b) depicts the predisposing factors of district Dhule, The annual rainfall value is about 0.6, the rainfall trend is at 1. The wet day frequency is at 0.1, the critical rainfall is at 0.2, the mean drought intensity is at 0 ,the drought magnitude is at 1 and the mean drought intensity is at 1 , the extreme drought intensity is at 0 the water availability is around 1, the total; water usage is at 1 . The population density is 0.1, the cultivable area is around 1, the net irrigated area is around 0.8,and the fertilizer consumption is at 0.8. Comparison of predisposing factors of districts (a) Beed& (b) Bhuldana is shown in Figure 15. Subplot 15 (a) depicts the predisposing factors of district Beed. The annual rainfall value is 0.8, the Rainfall trend is at 0.6, the wet day frequency is at 0.4, the critical rainfall is at 0.1, the mean drought intensity is at 0, the Drought magnitude is at 0.7, the extreme drought intensity is at 0.6, the severe drought intensity 0.3, the water usage value is at 1, the total water usage is at 1 and the cultivable area is around 0.1, the net irrigated is around 0.7, the fertilizer consumption is at 0.9. Subplot 15(b) depicts the predisposing factors of district Bhuldana. The annual Rainfall is at 1 the rainfall trend is at 0.2, the wet day frequency is at 1, the critical rainfall 0.1, the mean drought intensity is around 0.03, the Drought magnitude is at 0.9, the extreme drought intensity is at 0.2, the severe drought intensity is at 1. The average temperature is at 1 and the water availability is 1, is at 0.9, the total water usage is at 1. The income index 1 and the fertilizer consumption is at 0.6. Analysis of predisposing factors of districts (a) Jalna and (b)Aurangabad is shown in Figure 16. Subplot 16(a) depicts the predisposing factors of district Jalna. The annual rainfall is at 0.4, the rainfall trend is at 0.7 , the wet day frequency is at 0 the critical rainfall is at 0.4 ,the mean drought intensity is at 0, the drought magnitude is at 0.9, the extreme, drought intensity is at 0.6, the severe drought intensity is at 0.7 , the return period of extreme drought period is about 0.9, the returning period of extreme-drought period is about 1, the water availability is at 1, the total water usage is at 0.9 , the fertilizer consumption is at 0.6 . Subplot 16(b) depicts the predisposal factors of district Aurangabad. The annual rainfall is about 0.6 , the rainfall trend is about 0.8 ,the wet day frequency is t 0.1 ,the critical rainfall is about 0.2 , the mean drought intensity is about 0 the extreme drought intensity is about 0.4 , the severe drought intensity is about

1 , the returning period of severe-drought is about 1 ,the returning period of extreme-drought is about 1, the water availability is around 1, the total water usage is at 0.9, the net irrigated area is around 0.7 , the cultivable area is around 0.3 , the fertilizer consumption is around 0.7 . Analysis of predisposing factors of districts (a) Hingoli and (b) Parbhani is shown in Figure 17. Subplot 17(a) depicts the predisposing factors of district Hingoli the Annual Rainfall value is at 0.6, the rainfall trend is 0 and the wet day frequency is at 0.3 , the critical rainfall is at 0.3, the mean drought intensity is at 0 and the drought magnitude is at 0.1, the extreme drought intensity is at 0.3, the severe drought intensity is at 0 , the returning period of severe drought intensity is about 0 and the returning period of extreme drought intensity is about 0.7 , the Crop water demand is at 1 and the total water usage is about 0 and the fertilizer consumption is about 0.8 . Subplot 17(b) depicts the predisposing factors of district Parbhani. The annual rainfall is at 0.9 and the rainfall trend is around 0.3, the wet day frequency is at 0.8, the critical rainfall is around 0.1, the mean drought intensity is 0.04, the drought magnitude is about 0.8, the extreme drought intensity 0.2, and the severe drought intensity 0.7, the returning period of severe-drought 0.6 and the returning period of Severe-drought is about 0.9 and the potential evapotranspiration is at 0.8, the net sown area is around 0.9. The water availability is around 1 and the total water usage is around 0.9. The net irrigated area is around 0.8 and fertilizer consumption is around 0.9.

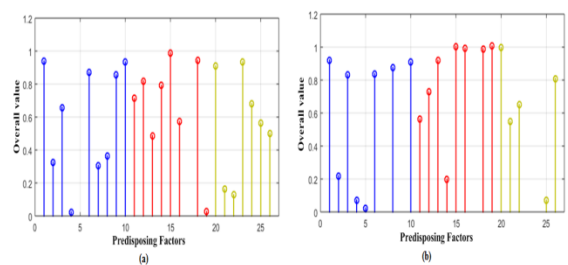


**Fig 8:** Comparison of predisposing factors of districts (a) Gadchiroli & (b) Gondia

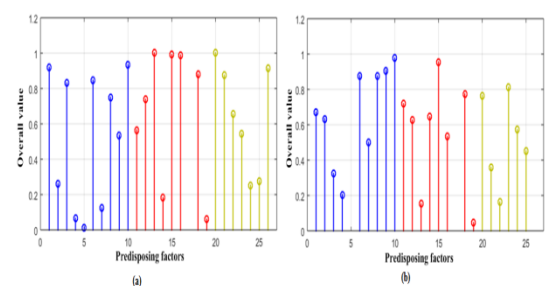


**Fig 9:** Analysis of predisposing factors of districts (a) Bhandara & (b) Chandrapur

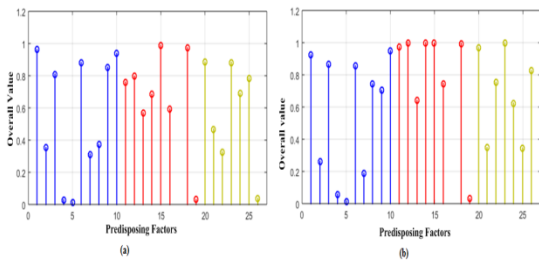


**Fig 10:** Comparison of predisposing factors of districts (a) Yavatmal & (b) Wardha

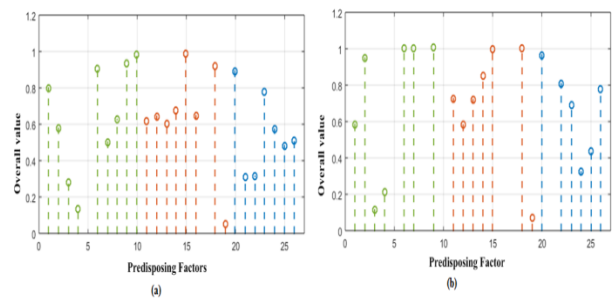


**Fig 14:** Analysis of predisposing factors of districts (a) Sindhudurg & (b) Dhule

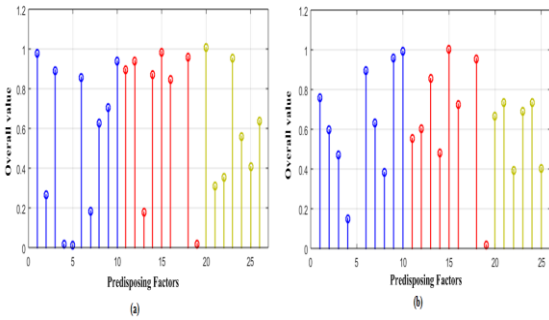


**Fig 11:** Analysis of predisposing factors of Districts (a) Osmanabad & (b) Latur

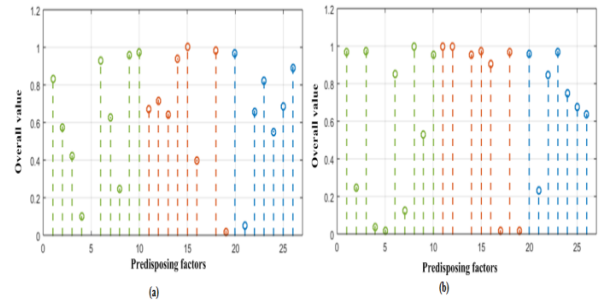


**Fig 15:** Comparison of predisposing factors of districts (a) Beed & (b) Bhuldana

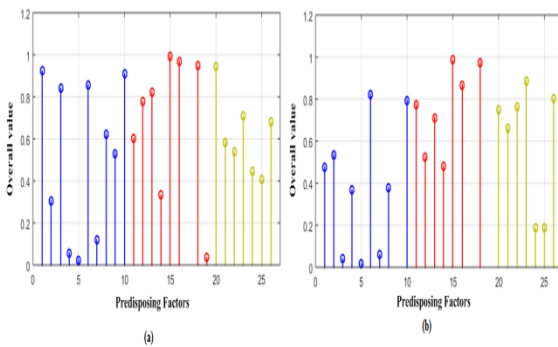


**Fig 12:** Analysis of predisposing factors of districts (a) Sangli & (b) Solapur

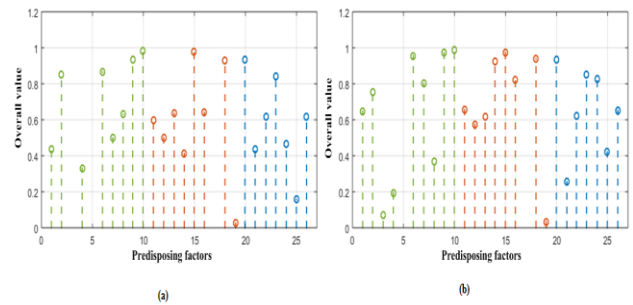


**Fig 16:** Analysis of predisposing Factors of districts (a) Jalna & (b) Aurangabad

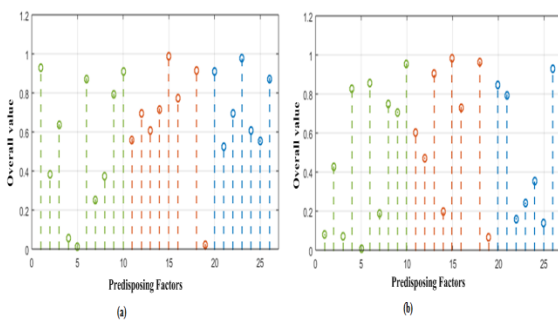


**Fig 13:** Analysis of predisposing factors at districts (a) jalgaon & (b) Ratnagiri

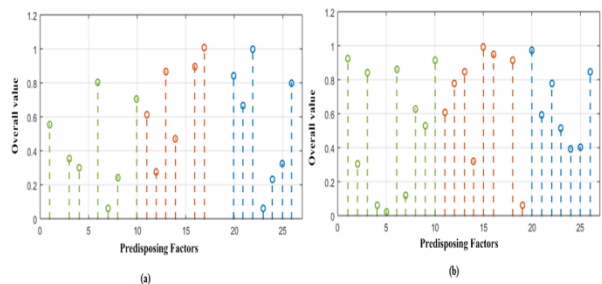


**Fig 17:** Analysis of predisposing factors of districts (a) Hingoli and (b) Parbhani

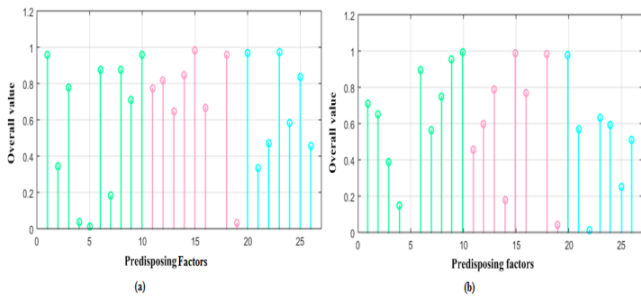


**Fig 18:** Analysis of predisposing Factors of districts (a) Nanded & (b) Akola

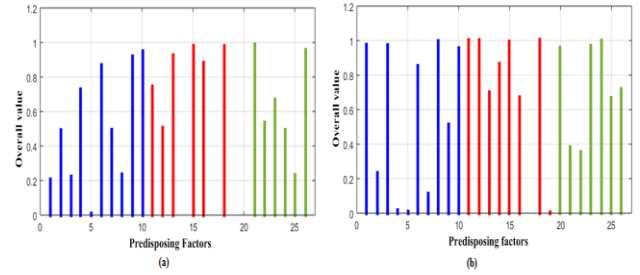


**Fig 22:** Analysis of predisposing factors of district (a) Nandurbar & (b) Palghar

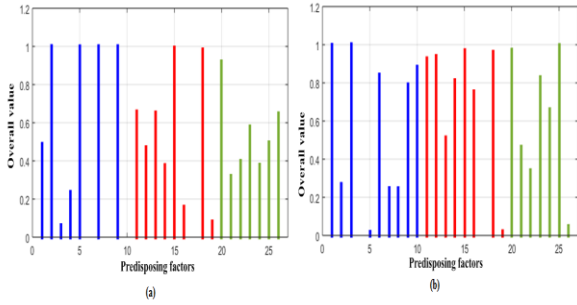


**Fig 19:** Analysis of predisposing Factors of districts (a) Amaravati & (b) Washim

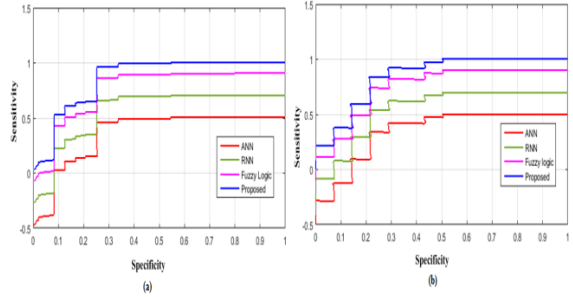


**Fig 23:** Comparison of Specificity and Sensitivity of the proposed algorithm (a) Success rate curve & (b) Prediction rate curve

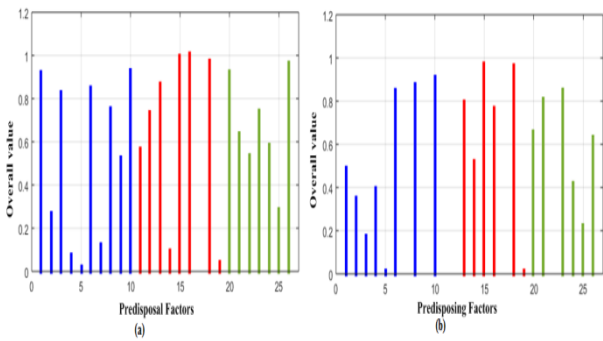


**Fig 20:** Analysis of predisposing factors of districts (a) Kolhapur & (b) Thane

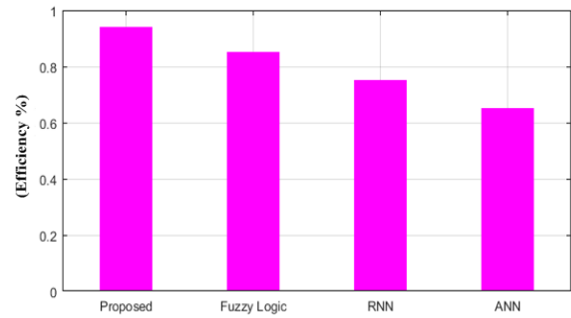


**Fig 24:** Analysis of (Efficiency %) in proposed and other Algorithms

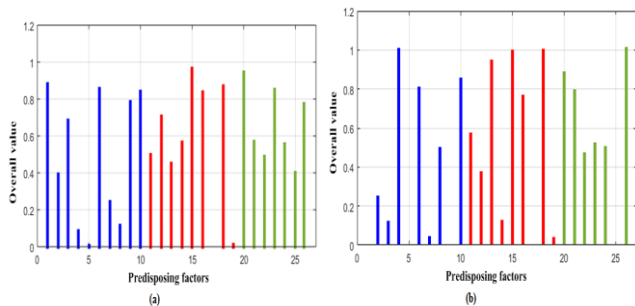


**Fig 21:** Comparison of predisposing factors of districts (a) Raigad & (b) Nagpur

Analysis of predisposing Factors of districts (a) Nanded & (b) Akola is shown in Figure 18. Subplot 18(a) depicts the predisposing factors of district Nanded. The annual rainfall value is at 0.9, the rain fall trend at 0.3, the wet day frequency is around 0.8, the critical rainfall 0.1 and the mean drought intensity is about 0.04. The Drought magnitude is around 0.9, the extreme drought intensity is around 0.9, the severe drought intensity is at 0.2 the value of return period of extreme drought is at 0.7, the returning period of severe-drought is 1 and the average temperature value is at 0.8, the net sown area is 0.9, the water availability is around 1 and the total water usage is around 1. And the net irrigated area is around 0.5, the fertilizer consumption value is at 0.5. Subplot 18(b) depicts the predisposing factors of district Akola. The Annual rainfall value is round 0.7, the rainfall trend is 0.6 and the wet day frequency is 0.4, The critical Rainfall is at 0.04, the mean

drought frequency is at 0 and the Drought magnitude is at 0.9, the extreme drought intensity is around 0.6, the severe drought intensity is at the value of 0.8 .the returning period of severe-drought index 0.9 and the returning period of extreme-drought index is at 1. The average temperature is at 0.5 and the potential evapotranspiration is at 0.7 and the net sown area is about 0.6 and the water availability is at 1 and the total water usage is around 1 .the net irrigated area is around 0.03. The fertilizer consumption is 0.5. Analysis of predisposing Factors of districts (a) Amaravati &(b) Washim is shown in Figure 19. Subplot 19(a) depicts the predisposal factors of district Amaravati. The annual rainfall value of the district is at 0.5. The rainfall trend is at 1 and the wet day frequency is at 1, the critical rainfall is around 0.2 and the mean drought intensity value is around 1, the drought magnitude is at 0 and the extreme drought intensity is about 0 the severe drought intensity is at 1. The returning period of severe-drought intensity is at 1 and the returning period of extreme-drought intensity 0. The Average temperature is around 0.7, the net sown area is around 0.5 and the water availability is 1 and the total water usage is also same as the water availability. The net irrigated area is at 0.4, the fertilizer consumption is around 0.7. Subplot 19 (b) depicts the predisposing factors of district Washim. The annual rainfall is around 1 and the rain fall trend is around 0.3 and the wet day frequency is at 0.1, the critical rainfall is around 0, the mean drought intensity is around 0.03 and the drought magnitude is about 0.8, the extreme drought intensity is a 0.3 and the severe drought intensity is at 0.3, and the returning period of severe-drought intensity is at 0.8and the returning period of extreme-drought intensity is at 0.9, the average temperature is at 0.9 and the water availability is at 1 and the total water usage is at 0.9, the net irrigated area is around 0.5, and the fertilizer consumption is at 0.1. Analysis of predisposing factors of districts (a) Kolhapur&(b) Thane is shown in Figure 20.Subplot 20(a) depicts the predisposing factors of district Kolhapur. The annual rainfall is about 0.9, the rain fall trend is about 0.3 and the wet day frequency is about 0.8, the critical rainfall is around 0.1, the mean drought intensity is at 0.04, the drought magnitude is around 0.9 and the extreme drought intensity is at 0.9 and the severe drought intensity is around 0.8, the returning period of severe-drought intensity is at 0.6, the value of severe drought intensity is 1, the water availability is at 1 and the total water usage of water is around 1. The fertilizer consumption is about 1. Subplot 20(b) depicts the predisposal factors of district thane. The annual rain fall is around 0.5 and the rainfall trend is at 0.4. The wet day frequency is at 0.2 and the critical rainfall is around 0.4 .the mean drought intensity 0.05. The drought magnitude is around 0.9 and the extreme drought intensity is around 0. The return period of severe drought intensity is around 0.9 the net sown area is around 0.8 and the water availability is around 1. The total water usage is around 1

and the fertilizer consumption is around 0.6.Comparison of predisposing factors of Districts (a) Raigad & (b) Nagpur is shown in Figure 21. Subplot 21(a) depicts the predisposing factors of district Raigad. The annual rain fall value is about 0.9, the rainfall trend is about 0.4 and the wet day frequency is around 0.7. The critical rain fall value is around 0.1. The mean drought intensity is around 0.04 and the drought magnitude is around 0.8, the extreme drought intensity is around 0.2 and the severe drought intensity is around 0.1. The returning period of severe-drought intensity is around 0.8 and the returning period of extreme-drought intensity is around 0.9. The water availability is at 1 and the total water usage 0.8. The net irrigated area is around 0.5 and the fertilizer consumption is around 0.8. Subplot 21(b) depicts the predisposing factors of district Nagpur. The annual rainfall trend is about 0.3 and the wet day frequency is about 0.1. The critical rainfall is about 1 and the drought magnitude is 0.8 and the return period of severe drought is around 0.9, the water availability of is about 1 and the total water usage is round 1. The fertilizer consumption is about 1. Analysis of predisposing factors of district (a) Nandurbar & (b) Palghar is shown in Figure 22. Subplot 22(a) depicts the predisposing factors of district Nandurbar. The annual rainfall value is about 0.2 and the rainfall trend is around 0.5. The wet day frequency is around 0.2and the critical rainfall is around 0.7. The mean drought intensity is around 0.04 and the drought magnitude is around 0.9. The extreme drought intensity is around 0.9 and the severe drought intensity is at 0.2 and the returning period of severe-drought intensity is around 0.9 and the returning period of extreme-drought intensity is around 1 and the water availability is around 1 and the total water usage is around 1 and the net irrigated area is around 0.4 and the fertilizer consumption is around 0.7.Subplot 22(b) depicts the predisposal factors of district Palghar. The annual rainfall value is around 1 and the rainfall trend is around 0.2. The wet day frequency is around 1 and the critical rainfall is around 0.03 and the mean drought intensity is around 0.9, the drought magnitude is around 0.9 and the extreme drought intensity is around 0.1 and the severe drought intensity is around 1 and the returning period of severe-drought intensity is about 0.5 and the returning period of extreme-drought intensity is around 1. The average temperature is around 1 and the water availability is around 1 and the total water usage is around 1 the net irrigated area is around 0.4 and the fertilizer consumption is around 0.7.Comparison of Specificity and Sensitivity of the proposed algorithm is shown in Figure 23. Subplot 23 (a) depicts the success rate curve of the proposed algorithm In ANN the Specificity starts from 0. And it reaches a high sensitivity of 0.5. The proposed algorithm starts from 0 and its sensitivity rises to a high value of 1 and it has more success rate than the other algorithms. Subplot 23(b) depicts the prediction curve rate of the proposed algorithm.

In RNN algorithm the specificity starts from 0 and its sensitivity rises to a high value of 0.5, In the proposed algorithm the Specificity starts from 0 and its sensitivity rises a high value of 1. By analyzing the above Figure (a) & (b) we can find the given proposed algorithm is better at prediction rate and success rate. Analysis of (Efficiency %) in proposed and other Algorithms is shown in Figure 24. The Efficiency of ANN is 0.6 and the efficiency of RNN is around 0.7 and the efficiency of Fuzzy logic is 0.8. Comparing all the above three algorithm we can simply find that the Efficiency of proposed algorithm is at 0.9 that is way better than the other methods.

## 6. Conclusion

This paper, the Spiking Neural Network Based Water management in Drought area of Maharashtra India is studied with the help of proposed Spiking neural network. The proposed method performance is investigated in the MATLAB platform and compared with existing approaches. The performance of proposed and existing techniques is graphically demonstrated. The proposed method helps to successfully predict the drought and the proposed method illustrates the predisposing factors of the drought prone district of Maharashtra. The proposed method is way better in predicting the drought and it has more successful rate than the existing methods the efficiency of the proposed technique is way much higher than the existing methods like ANN, RNN and Fuzzy logic, the results attained from the simulation study reveals that the proposed method performs better than the existing approaches.

## References

- [1] A. AghaKouchak, A. Farahmand, F. S. Melton, J. Teixeira, M. C. Anderson, B. D. Wardlow, and C. R. Hain, 2015. Remote sensing of drought: Progress, challenges and opportunities. *Reviews of Geophysics*, 53(2), pp.452-480.
- [2] J. Bai, Q. Cui, D. Chen, H. Yu, X. Mao, L. Meng, and Y. Cai, 2018. Assessment of the SMAP-derived soil water deficit index (SWDI-SMAP) as an agricultural drought index in China. *Remote Sensing*, 10(8), p.1302.
- [3] J. P. Bloomfield and B. P. Marchant, 2013. Analysis of groundwater drought building on the standardised precipitation index approach. *Hydrology and Earth System Sciences*, 17(12), pp.4769-4787.
- [4] K. Devdatta Mokashi, and Prof. (Dr.) Vidula S. Sohoni, 2021. Identification of Water Conservation Zone By Application Of Electrical Resistivity Method In Parts of Osmanabad District, Maharashtra-India, *International Journal of Engineering Trends and Technology*, 69(3), pp.233-238.
- [5] T. Che, X. Li, R. Jin, R. Armstrong, and T. Zhang, 2008. Snow depth derived from passive microwave remote-sensing data in China. *Annals of Glaciology*, 49, pp.145-154.
- [6] Y. Chen, K. Yang, J. He, J. Qin, J. Shi, J. Du, and Q. He, 2011. Improving land surface temperature modeling for dry land of China. *Journal of Geophysical Research: Atmospheres*, 116(D20).
- [7] R. Li, A. Tsunekawa, and M. Tsubo, 2014. Index-based assessment of agricultural drought in a semi-arid region of Inner Mongolia, China. *Journal of Arid Land*, 6, pp.3-15.
- [8] F. N. Kogan, 1990. Remote sensing of weather impacts on vegetation in non-homogeneous areas. *International Journal of remote sensing*, 11(8), pp.1405-1419.
- [9] M. Kędzior and J. Zawadzki, 2016. Comparative study of soil moisture estimations from SMOS satellite mission, GLDAS database, and cosmic-ray neutrons measurements at COSMOS station in Eastern Poland. *Geoderma*, 283, pp.21-31.
- [10] G. Wong, H. A. J. van Lanen, and P. J. J. F. Torfs. 2013. Probabilistic analysis of hydrological drought characteristics using meteorological drought. *Hydrological Sciences Journal*, 58(2), pp.253-270.
- [11] A. K. Qin, V. L. Huang, and P. N. Suganthan, 2008. Differential evolution algorithm with strategy adaptation for global numerical optimization. *IEEE transactions on Evolutionary Computation*, 13(2), pp.398-417.
- [12] B. Sivakumar, 2011. Global climate change and its impacts on water resources planning and management: assessment and challenges. *Stochastic Environmental Research and Risk Assessment*, 25, pp.583-600.
- [13] S. Adarsh and M. Janga Reddy, 2015. Trend analysis of rainfall in four meteorological subdivisions of southern India using nonparametric methods and discrete wavelet transforms. *International journal of Climatology*, 35(6), pp.1107-1124.
- [14] P. Guhathakurta, and E. Saji, 2013. Detecting changes in rainfall pattern and seasonality index vis-à-vis increasing water scarcity in Maharashtra. *Journal of Earth System Science*, 122, pp.639-649.
- [15] J. Fito, N. Tefera, S. Demeku, and H. Kloos, 2017. Water footprint as an emerging environmental tool for assessing sustainable water use of the bioethanol distillery at Metahara sugarcane farm, Oromiya Region, Ethiopia. *Water Conservation Science and Engineering*, 2, pp.165-176.
- [16] A. Yinglan, G. Wang, T. Liu, S. Shrestha, B. Xue, and Z. Tan, 2019. Vertical variations of soil water and its



controlling factors based on the structural equation model in a semi-arid grassland. *Science of the Total Environment*, 691, pp.1016-1026.

- [17] J. Rhee, J. Im, and G. J. Carbone, 2010. Monitoring agricultural drought for arid and humid regions using multi-sensor remote sensing data. *Remote Sensing of environment*, 114(12), pp.2875-2887.
- [18] K. E. Saxton and W. J. Rawls, 2006. Soil water characteristic estimates by texture and organic matter for hydrologic solutions. *Soil science society of America Journal*, 70(5), pp.1569-1578.
- [19] W. Shangguan, Y. Dai, Q. Duan, B. Liu, and H. Yuan, 2014. A global soil data set for earth system modeling. *Journal of Advances in Modeling Earth Systems*, 6(1), pp.249-263.
- [20] S. Shukla and A. W. Wood, 2008. Use of a standardized runoff index for characterizing hydrologic drought. *Geophysical research letters*, 35(2).
- [21] P. C. Spennemann, J. A. Rivera, A. C. Saulo, and O. C. Penalba, 2015. A comparison of GLDAS soil moisture anomalies against standardized precipitation index and multisatellite estimations over South America. *Journal of Hydrometeorology*, 16(1), pp.158-171.
- [22] K. Zhou, J. Li, T. Zhang, and A. Kang.2021. The use of combined soil moisture data to characterize agricultural drought conditions and the relationship among different drought types in China. *Agricultural Water Management*, 243, p.106479.
- [23] M. I. Hossain, M. N. Bari, S. U. Miah, A.-Kafy, and N. M. R. Nasher, 2021. Application of modified managed aquifer recharge model for groundwater management in drought-prone water-stressed Barind Tract, Bangladesh. *Environmental Challenges*, 4, p.100173.
- [24] M. Hiloidhari, V. Vijay, R. Banerjee, D. C. Baruah, and A. B. Rao, 2021. Energy-carbon-water footprint of sugarcane bioenergy: A district-level life cycle assessment in the state of Maharashtra, India. *Renewable and Sustainable Energy Reviews*, 151, p.111583.
- [25] N. Neeti, C. M. ArunMurali, V. M. Chowdary, N. H. Rao, and M. Kesarwani, 2021. Integrated meteorological drought monitoring framework using multi-sensor and multi-temporal earth observation datasets and machine learning algorithms: A case study of central India. *Journal of Hydrology*, 601, p.126638.
- [26] P. Quintana-Seguí, A. Barella-Ortiz, S. Regueiro-Sanfiz, and G. Miguez-Macho, 2020. The utility of land-surface model simulations to provide drought information in a water management context using global and local forcing datasets. *Water Resources Management*, 34, pp.2135-2156.
- [27] S. M. Ahmed, 2020. Impacts of drought, food security policy and climate change on performance of irrigation schemes in Sub-saharan Africa: The case of Sudan. *Agricultural Water Management*, 232, p.106064.
- [28] S. Nandi and J. R. Manne, 2020. Spatiotemporal analysis of water balance components and their projected changes in near-future under climate change over Sina Basin, India. *Water Resources Management*, 34, pp.2657-2675.
- [29] S. Adarsh and M. Janga Reddy, 2015. Trend analysis of rainfall in four meteorological subdivisions of southern India using nonparametric methods and discrete wavelet transforms. *International journal of Climatology*, 35(6), pp.1107-1124.
- [30] A. Ahmadalipour, H. Moradkhani, and M. Svoboda, 2017. Centennial drought outlook over the CONUS using NASA-NEX downscaled climate ensemble. *International Journal of Climatology*, 37(5), pp.2477-2491.
- [31] Y. Bao and X. Wen, 2017. Projection of China's near-and long-term climate in a new high-resolution daily downscaled dataset NEX-GDDP. *Journal of Meteorological Research*, 31(1), pp.236-249.
- [32] S. N. Gosling, R. G. Taylor, N. W. Arnell, and M. C. Todd, 2011. A comparative analysis of projected impacts of climate change on river runoff from global and catchment-scale hydrological models. *Hydrology and Earth System Sciences*, 15(1), pp.279-294.
- [33] W. O. Ochola and P. Kerkides, 2003. A Markov chain simulation model for predicting critical wet and dry spells in Kenya: analysing rainfall events in the Kano Plains. *Irrigation and Drainage: The journal of the International Commission on Irrigation and Drainage*, 52(4), pp.327-342.
- [34] X. Liang, D. P. Lettenmaier, E. F. Wood, and S. J. Burges, 1994. A simple hydrologically based model of land surface water and energy fluxes for general circulation models. *Journal of Geophysical Research: Atmospheres*, 99(D7), pp.14415-14428.
- [35] J. Abolverdi and D. Khalili, 2010. Probabilistic analysis of extreme regional meteorological droughts by L-moments in a semi-arid environment. *Theoretical and Applied Climatology*, 102, pp.351-366.
- [36] D. C. Edossa, M. S. Babel, and A. Das Gupta, 2010. Drought analysis in the Awash river basin, Ethiopia. *Water resources management*, 24, pp.1441-1460.
- [37] V. K. Lohani and G. V. Loganathan, 1997. An early warning system for drought management using the

- palmer drought index 1. *JAWRA Journal of the American Water Resources Association*, 33(6), pp.1375-1386.
- [38] V. K. Lohani, G. V. Loganathan, and S. Mostaghimi, 1998. Long-term analysis and short-term forecasting of dry spells by Palmer Drought Severity Index. *Hydrology Research*, 29(1), pp.21-40.
- [39] Verma, R. ., Dhanda, N. ., & Nagar, V. . (2023). Analysing the Security Aspects of IoT using Blockchain and Cryptographic Algorithms. *International Journal on Recent and Innovation Trends in Computing and Communication*, 11(1s), 13–22. <https://doi.org/10.17762/ijritcc.v11i1s.5990>
- [40] A. K. Mishra, V. R. Desai, and V. P. Singh, 2007. Drought forecasting using a hybrid stochastic and neural network model. *Journal of Hydrologic Engineering*, 12(6), pp.626-638.
- [41] R. Modarres, 2010. Regional dry spells frequency analysis by L-moment and multivariate analysis. *Water resources management*, 24(10), pp.2365-2380.
- [42] S. Morid, V. Smakhtin, and M. Moghaddasi, 2006. Comparison of seven meteorological indices for drought monitoring in Iran. *International Journal of Climatology: A Journal of the Royal Meteorological Society*, 26(7), pp.971-985.
- [43] M. Abedinpour, A. Sarangi, T. B. S. Rajput, M. Singh, H. Pathak, and T. Ahmad, 2012. Performance evaluation of AquaCrop model for maize crop in a semi-arid environment. *Agricultural Water Management*, 110, pp.55-66.
- [44] C. Accadia, S. Mariani, M. Casaioli, A. Lavagnini, and A. Speranza, 2005. Verification of precipitation forecasts from two limited-area models over Italy and comparison with ECMWF forecasts using a resampling technique. *Weather and Forecasting*, 20(3), pp.276-300.
- [45] Mondal , D. (2021). Green Channel Roi Estimation in The Ovarian Diseases Classification with The Machine Learning Model . *Machine Learning Applications in Engineering Education and Management*, 1(1), 07–12.
- [46] A.Arabameri, O.AsadiNalivan, S. Chandra Pal, R.Chakraborty, A.Saha, S. Lee, B.Pradhan, and TienD.Bui, 2020. Novel machine learning approaches for modelling the gully erosion susceptibility. *Remote Sensing*, 12(17), p.2833.
- [47] K. Chandrasekar, M. V. Sai, P. S. Roy, V. Jayaraman, and R. R. Krishnamurthy, 2009. Identification of agricultural drought vulnerable areas of Tamil Nadu, India--using GIS based multi criteria analysis. *Asian Journal of Environment and Disaster Management*, 1(1).
- [48] H. Chen, S.Guo, C.-yuXu, and V. P. Singh, 2007. Historical temporal trends of hydro-climatic variables and runoff response to climate variability and their relevance in water resource management in the Hanjiang basin. *Journal of hydrology*, 344(3-4), pp.171-184.
- [49] J. Cheng and J.-ping Tao, 2010. Fuzzy comprehensive evaluation of drought vulnerability based on the analytic hierarchy process:—an empirical study from Xiaogan City in Hubei Province. *Agriculture and Agricultural Science Procedia*, 1, pp.126-135.
- [50] S. S. Cooley, C. A. Williams, J. B. Fisher, G. H. Halverson, J. Perret, and C. M. Lee, 2019. Assessing regional drought impacts on vegetation and evapotranspiration: a case study in Guanacaste, Costa Rica. *Ecological applications*, 29(2), p.e01834.
- [51] K. L. Ebi and K. Bowen, 2016. Extreme events as sources of health vulnerability: Drought as an example. *Weather and climate extremes*, 11, pp.95-102.
- [52] A. Gayen, S. M. Haque, and S. Saha, 2020. Modeling of gully erosion based on random forest using GIS and R. *Gully Erosion Studies from India and Surrounding Regions*, pp.35-44.
- [53] C. Liu, W. Shen, L. Zhang, Y. Du, and Z. Yuan, 2021. Spike neural network learning algorithm based on an evolutionary membrane algorithm. *IEEE Access*, 9, pp.17071-17082.